Advances in Machinery, Materials Science and Engineering Application
M. Chen et al. (Eds.)

doi:10.3233/ATDE220433

Enhancement Mechanical Properties of B_4C Ceramics with the Core-Shell Structure Powders

Wankai YAO [a], Junbin YAN [b], Xiangcheng LI [a,1], Pingan CHEN [a] and Boquan Zhu [a]
[a] *The State Key Laboratory of Refractories and Metallurgy, Wuhan University of Science and Technology, Wuhan, China*
[b] *Wuhan Xinxin Semiconductor Manufacturing Co., Ltd, Wuhan, China*

Abstract. In order to improve the mechanical properties of B_4C ceramics, $B_4C@TiB_2$ composite powders with core-shell structure are prepared by molten salt method using B_4C and Ti powders as raw materials. And B_4C ceramics were prepared from $B_4C@TiB_2$ composite powders by spark plasma sintering (SPS). The results show that the $B_4C@TiB_2$ composite powders exhibit intact core-shell structure. The $B_4C@TiB_2$ composite powders improves the mass transfer during spark plasma sintering. When the molar ratio of B_4C/Ti is 2/1, the relative density, Vickers hardness, fracture toughness and flexural strength of the BT1/2 sample are 94.2%, 26.9 GPa, 5.34 MPa·$m^{1/2}$ and 570 MPa, respectively, which is best comprehensive properties.

Keywords. Core-shell structure, boron carbide (B_4C) ceramics, spark plasma sintering (SPS), reinforcing and toughing

1. Introduction

Boron carbide (B_4C) ceramics have high melting point, ultrahigh hardness, high elastic modulus, low specific density, good wear resistance as well as excellent high temperature and chemical stability [1]. Therefore, the B_4C ceramics can be widely used in bulletproof materials, refractory materials, wear-resistant materials, self-lubricating materials, especially acid-resistant materials, cutting and grinding tools, atomic reactor control and shielding materials, etc [2]. However, the sintering performance of pure boron carbide is poor, which the sintering temperatures of B_4C ceramics for densification are almost higher than 2000 °C. In addition, the low fracture toughness of B_4C ceramics limits their further application [3].

The addition of second phase can effectively improve the strength and toughness of the B_4C ceramics. Among them, titanium boride (TiB_2) with ultrahigh hardness and high melting point has attracted much attention of many researchers [4, 5]. The hardness of TiB_2 can reach 25~32 GPa, which is higher than that of other transition metal diborides such as ZrB_2(22.1 GPa) and HfB_2 [6]. Therefore, TiB_2 as the second phase in the B_4C ceramic helps to maintain the high hardness as well as improving the sintering behavior [7]. At the same time, TiB_2 has a lower density (4.52 g/cm^3) than

[1] Xiangcheng Li, Corresponding author, The State Key Laboratory of Refractories and Metallurgy, Wuhan University of Science and Technology, Wuhan, China; E-mail: lixiangcheng@wust.edu.cn.

other transition metal diborides such as ZrB_2 (6.09 g/cm^3) and HfB_2 (10.5 g/cm^3) [8, 9]. In addition, TiB_2 has a higher thermal expansion coefficient than other transition metal diborides, such as ZrB_2, TaB_2 and HfB_2. The thermal stress generated between TiB_2 and B_4C can improve the fracture toughness of B_4C ceramics [10].

In order to improve the mechanical properties of B_4C ceramics, the B_4C@TiB_2 composite powders are obtained by molten salt method in this paper, which the TiB_2 shell is in-situ formed on the surface of B_4C powders. Subsequently, B_4C@TiB_2 composite powders are sintered by SPS. The effects of different B_4C/Ti molar ratios on the microstructure and mechanical properties of B_4C ceramics are investigated.

2. Experiment

2.1. Sample Preparation

B_4C powder (20 μm, analytically pure) and Ti powder (1~3 μm, purity>99.9%) are used as raw materials. KCl and NaCl (analytically pure) are used as raw materials of molten salt. The raw materials are weighed according to the molar ratio of B_4C:Ti=1:1, 1:1/2, 1:1/4, 1:1/6, and pure B_4C are used as the control group. The mixture is obtained according to the mass ratio of KCl:NaCl=1:1 and (KCl+NaCl):(B_4C+Ti)=5:1. This mixture is heated in a tube furnace at 1100 ºC in a flowing Ar atmosphere for 4 h to form TiB_2 on the surface of B_4C powders. Then, the obtained product is wished with water and anhydrous ethanol for many times until there is no salt, and the B_4C@TiB_2 composite powders are obtained after drying. Finally, the sintering process is carried out by spark plasma sintering in a vacuum atmosphere. The maximum temperature is 1700 °C for 6 min, and a pressure of 50 MPa is applied throughout the process.

2.2. Characterizations

The phase compositions of samples are characterized by X-ray diffractometer (XRD). The microscopic morphology of the B_4C@TiB_2 composite powders and B_4C ceramics are analyzed using a field emission scanning electron microscope (FESEM). Bulk density is measured using the Archimedes method. Vickers hardness and fracture toughness are measured by the indentation method, using a Vickers hardness tester with an indenter made of diamond and an angle of 136° on the polished surface for 15 s under a load of 5 kg. The bending strength is measured using the three-point bending method.

3. Results and Discussions

3.1. Phase Diagram Analysis of B4C@TiB2 Composite Powders

The phase analysis of the B_4C@TiB_2 composite powders is carried out by XRD, and the results are shown in figure 1. It can be seen that the B_4C@TiB_2 composite powders are mainly composed of B_4C, TiB_2 and a small amount of TiC, and no residual Ti is detected, indicating that Ti has reacted with B_4C in the molten salt. The intensity of TiB_2 diffraction peak increases with the Ti amount, while the intensity of B_4C

diffraction peak is just the opposite. The existence of the TiC diffraction peak in the BT1 sample is due to the excessive amount of Ti, and the generated TiC has not completely converted into TiB_2. In the subsequent discharge plasma sintering, the residual TiC will continue to react with B_4C to form TiB_2.

From the results of XRD, Ti and B_4C to form B_4C@TiB_2 composite powders with core-shell structure in the molten salt at 1100 °C. The molten salt promotes the dissolution of Ti and makes Ti exist in the form of "naked" ions, which effectively reduces the reaction barrier and temperature of the reaction between B_4C and Ti. And mass transfer in the molten salt between B_4C and Ti ensures the uniform nucleation and growth of TiB_2 on the surface of B_4C particles.

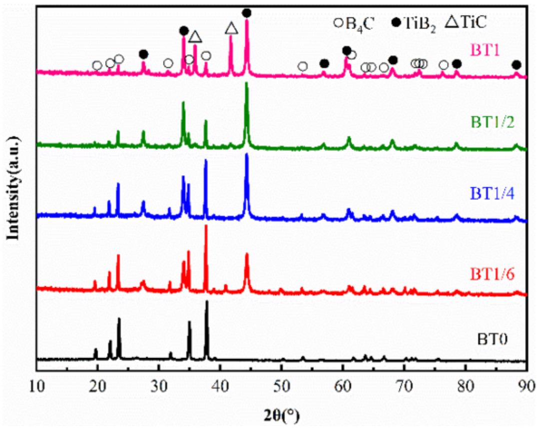

Figure 1. XRD patterns of B_4C@TiB_2 composite powders.

3.2. *Microstructure of B_4C ceramics*

The BSE images of B_4C ceramics are shown in figure 2. Figure 2(a) shows the polished surface of the BT0 sample, the light color phase is B_4C, and the black color represents the pores. From figure 2 (a), there are a large number of pores in the sample, indicating that the sintered compactness of pure B_4C powder is poor. It can be seen from figures 2(b)~(e) that the gray phase is B_4C, and the white phase is TiB_2. Compared with the control group BT0, the pores are significantly reduced. It shows that the B_4C@TiB_2 composite powders can effectively reduce the sintering temperature of B_4C ceramics. The TiB_2 phase forms an interconnected network structure that wraps the B_4C grains in a cage-like structure, which can restrain the movement and growth of B_4C grain boundaries by pinning during the sintering process.

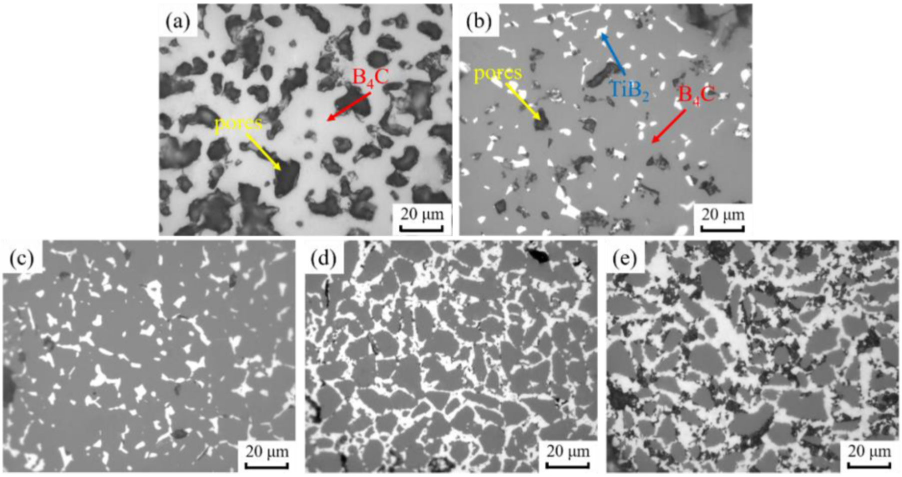

Figure 2. BSE image of B_4C ceramics. (a)BT0, (b)BT1/6, (c)BT1/4, (d)BT1/2, (e)BT1.

3.3. Mechanical Properties of B_4C Ceramics

The relative density and bulk density of B_4C ceramics are shown in figure 3(a). The relative density of the BT0 sample is 82.1%, while the relative density of BT1/6 sample reaches 95.4%, with an increase of 16.2%. The bulk densities of B_4C ceramics increase from 2.07 g/cm^3 to 3.20 g/cm^3. It indicates that the sintering performance of B_4C Ceramics can be significantly improved by coating TiB_2 on the surfaces of B_4C powders. It can be seen from figures 3(b)~(c) that B_4C ceramics prepared from $B_4C@TiB_2$ composite powders can effectively improve their mechanical properties. And when the molar ratio of B_4C/Ti is 2/1, the Vickers hardness, fracture toughness and flexural strength of the BT1/2 sample are 26.9 GPa, 5.34 MPa·m$^{1/2}$ and 570 MPa, respectively, which is best comprehensive properties.

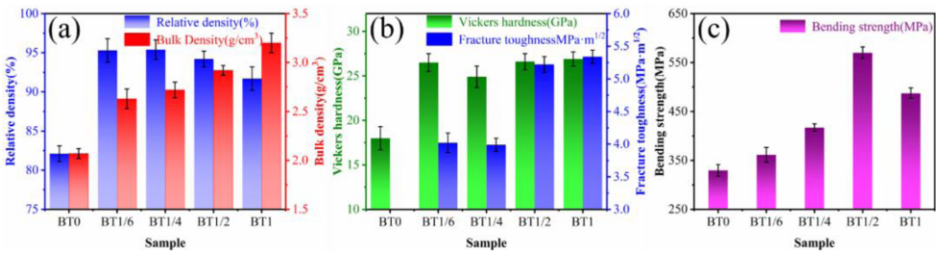

Figure 3. Mechanical properties of B_4C ceramics. (a) Relative density and bulk density, (b) Vickers hardness and fracture toughness, (c) Flexural strength.

3.4. Toughening Mechanism of B_4C Ceramics

The crack propagation of BT1/2 sample after Vickers hardness indentation is shown in figure 4. There are obvious crack deflection, crack bridging and crack branching in the B_4C ceramics. These mechanisms increase fracture toughness by consuming more of the energy required for fracture. In addition, the fracture mode of B_4C ceramics are transformed into a hybrid mode of intergranular and transgranular fracture, which is beneficial for the improvement of fracture toughness.

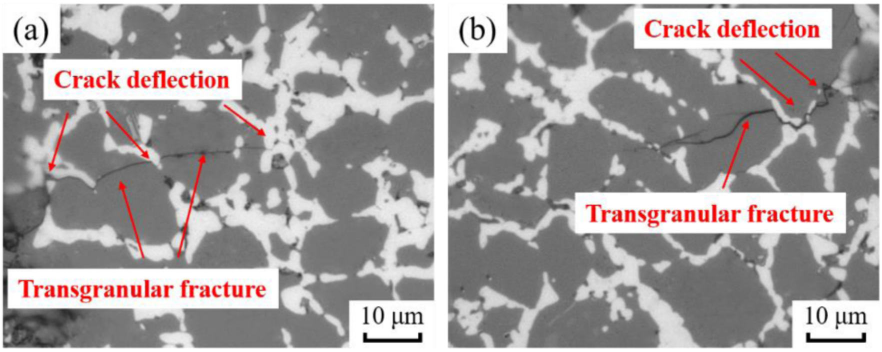

Figure 4. Vickers indentation crack propagation paths of BT1/2.

4. Conclusions

In this study, the $B_4C@TiB_2$ composite powders with core-shell structure is obtained by molten salt method. The TiB_2 phase is evenly distributed on the surface of B_4C, forming a uniform and dense coating structure. The $B_4C@TiB_2$ composite powders improves the mass transfer during SPS. The TiB_2 phase could form a cage-like structure to wrap the B_4C grains hinder the growth of B_4C grains by pinning. When the molar ratio of B_4C/Ti is 2/1, the Vickers hardness, fracture toughness and flexural strength of the BT1/2 sample are 26.9 GPa, 5.34 MPa·m$^{1/2}$ and 570 MPa, respectively, which is best comprehensive properties.

Acknowledgements

This work is supported by the Science Fund for Creative Research Groups of the National Natural Science Foundation of Hubei Province (Grant No.2020CFA038), the Key Research and Development Project of Hubei Province (Grant No. 2020BAA028).

References

[1] Song N, Gao Z, Zhang Y, Li X. B_4C nanoskeleton enabled, flexible lithium-sulfur batteries. Nano Energy. 2019; 58:30-9.
[2] Reddy KM, Guo D, Song S, Cheng C, Han J, Wang X, et al. Dislocation-mediated shear amorphization in boron carbide. Sci. Adv. 2021;7(8): eabc6714.
[3] Suri A, Subramanian C, Sonber J, Murthy TC. Synthesis and consolidation of boron carbide: A review. Int. Mater. Rev. 2010; 55(1):4-40.
[4] Dai FZ, Xiang H, Zhou Y. Strategy to design high performance TiB_2-based materials: Strengthen grain boundaries by solid solute segregation. J. Am. Ceram. Soc. 2020; 103(5):3311-20.
[5] Liu C, Zhang Z, Yang G, Zhou A, Wang G, Qin S, et al. Finite element analysis and wear mechanism of B_4C-TiB_2 ceramic tools in turning AISI 4340 workpieces. Ceram. Int. 2022;48(4):5459-67.
[6] Ren D, Deng Q, Wang J, Yang J, Li Y, Shao J, et al. Synthesis and properties of conductive B_4C ceramic composites with TiB_2 grain network. J. Am. Ceram. Soc. 2018; 101(9):3780-6.

[7] Khajehzadeh M, Ehsani N, Baharvandi HR, Abdollahi A, Bahaaddini M, Tamadon A. Thermodynamical evaluation, microstructural characterization and mechanical properties of B_4C-TiB_2 nanocomposite produced by in-situ reaction of nano-TiO_2. Ceram. Int. 2020; 46(17):26970-84.
[8] Zhang M, Ren X, Zhang M, Wang S, Wang L, Yang Q, et al. Preparation of ZrB_2-$MoSi_2$ high oxygen resistant coating using nonequilibrium state powders by self-propagating high-temperature synthesis. J Adv. Ceram. 2021; 10(5):1011-24.
[9] Zhang X, Zhang Z, Liu Y, Wang A, Tian S, Wang W, et al. High-performance B_4C-TiB_2-SiC composites with tuneable properties fabricated by reactive hot pressing. J. Eur. Ceram. Soc. 2019; 39(10):2995-3002.
[10] Liu D, Fu Q, Chu Y. Molten salt synthesis, formation mechanism, and oxidation behavior of nanocrystalline HfB_2 powders. J. Adv. Ceram. 2020; 9(1):35-44.